Chattering-Free Adaptive Wavelet Neural Network Controller Design for a Class of Nonlinear Systems

Chun-Fei Hsu

***Abstract*—In order to ensure the conventional adaptive wavelet neural network control systems' stability, a compensator could be designed to dispel the approximation error. The most frequently used of compensator is like a sliding-mode control which maybe cause chattering phenomena to wear the bearing mechanism. To tackle this problem, this paper proposes a chattering-free adaptive wavelet neural network control (CAWNNC) system. The proposed CAWNNC system is composed of a neural controller and a smooth compensator. The neural control uses a fuzzy wavelet neural network to online approximate an ideal controller and the smooth compensator is used to remove the chattering phenomena of conventional sliding-mode control completely. Then, the proposed CAWNNC approach is applied to two chaotic nonlinear systems to investigate its effectiveness. Through the simulation results, the proposed CAWNNC scheme can achieve favorable tracking performance and the convergence of the tracking error and control parameters can be accelerated by the developed PI adaptation learning algorithm.**

***Keywords*—Adaptive control, neural control, chaotic system, wavelet neural network.**

I. Introduction

From the control point of view, if the exact model of the controlled system is well known, there exists an ideal controller scheme to achieve favorable control performance by canceling all the system dynamics [1]. However, a tradeoff between system stability and model accuracy is necessary for the performance of ideal controller. To relax this requirement, a sliding-mode control strategy offers a number of attractive properties for the tracking control, such as insensitivity to parameter variations, external disturbance rejection and fast dynamic responses [1]. However, the chattering phenomena of the sliding mode control will wear the bearing mechanism.

Many control systems in practice have either partially unknown or completely unknown nonlinearities. To tackle the above problem, some model-free neural-network-based adaptive control systems have been developed to deal with the control problems of such nonlinear uncertain systems [2]-[6]. Using optimization technique (gradient method), the parameters of neural network are tuned offline to minimize the approximation error. A limitation of this approach is its offline nature. In real time control, it would be hard to continuously tune neural network so as to improve the system performance. The most useful property is their ability of neural networks can approximate arbitrary linear or nonlinear mapping through learning. By adequately choosing neural network structures, training methods and sufficient input data, the neural-network-based adaptive controllers are capable to compensate for the effects of nonlinearities and system uncertainties [2].

Recently, to achieve better learning performance of neural network, some researchers have combined the layered structure of neural network and the wavelet functions to construct the wavelet neural network (WNN) [7]-[9]. Unlike the sigmoidal functions used in conventional neural networks, wavelet functions are spatially localized, so that the learning capability of WNN is more efficient than the conventional sigmoidal function neural network [7]. Wavelets have become a very active subject in many scientific and engineering research areas. Especially, WNN inspired by both the feedforward neural networks and wavelet decompositions have received considerable attention and become a popular tool for function approximation [9].

There have been many considerable interests in exploring the applications of WNN to deal with unknown nonlinearity control systems [10]-[14]. These WNN-based adaptive controllers combine the capability of artificial neural networks for learning ability and the capability of wavelet decomposition for identification ability. Though the WNN-based adaptive controller can achieve favorable tracking performance [10]-[14], in order to ensure the systems' stability, a compensation controller could be designed to dispel the approximation error. The most frequently used of compensation controller is like a sliding-mode control, which requires the bound of the approximation error [11], [14]. If the bound of approximation error is chosen too small, the system stabilization can not guarantee. However, if the bound of approximation error is chosen too large, the control effort will cause chattering phenomena to wear the bearing mechanism.

To tackle this problem, an approximation error bound estimation mechanism is investigated to estimate the bound of approximation error so that the chattering phenomenon of the control effort can be reduced [15]. However, the adaptive law for the estimation error bound will make it go to infinity. Some researchers have proposed neural-network-based adaptive control design methods based on the H^{∞} control

Manuscript received June 4, 2009. This work was supported in part by the National Science Council of Republic of China under grant NSC 97-2221-E-216-029.

C. F. Hsu is with the Department of Electrical Engineering, Chung Hua University, Hsinchu 300, Taiwan, Republic of China (phone: 886-3-5186399; fax: 886-3-5186436; e-mail: fei@chu.edu.tw).

scheme [16]-[18]. Combing the H^{∞} control, these neural-network-based robust adaptive control approaches can attenuate the effects of approximation error to a prescribed level. However, it is a trade-off between the amplitude of control effort and the performance of tracking error by choosing the specified attenuation level.

This paper proposed a chattering-free adaptive wavelet neural network control (CAWNNC) system. The proposed CAWNNC system consists of a neural controller and a smooth compensator. The neural controller utilizes a fuzzy wavelet neural network (FWNN) to online mimic an ideal controller using a PI type adaptation learning algorithm, and the smooth compensator uses a fuzzy system to remove the chattering phenomena on conventional sliding-mode control completely. In addition, the learning algorithm is derived based on the Lyapunov function to guaranteed system's stability and the Taylor linearization technique is employed to increase the learning ability of FWNN. Finally, the proposed CAWNNC approach is applied to two chaotic nonlinear systems to investigate the effectiveness. Some simulation results are provided to verify the effectiveness of the developed CAWNNC scheme.

II. Problem Formulation

Consider a class of *n*-th order chaotic systems described by the following form

$$x^{(n)} = f(\mathbf{x}) + u \tag{1}$$

where $\mathbf{x} = [x, \dot{x}, \ldots, x^{(n-1)}]^T \in R^n$ is the state vector of the system, which is assumed to be available for measurement, $f(\mathbf{x}) \in R$ is the nonlinear system dynamics which can be unknown, and $u \in R$ is the input of the system. The control objective of chaotic system is to find a control law so that the state trajectory x can track a trajectory command x_c. A tracking error is defined as

$$e = x_c - x . \tag{2}$$

If the system dynamic function is well known, there exits an ideal controller as [1]

$$u^* = -f(\mathbf{x}) + x_c^{(n)} + k_1 e^{(n-1)} + \cdots + k_{n-1}\dot{e} + k_n e \tag{3}$$

where $k_i, i = 1,2,...,n$ are the non-zero constants. Apply the ideal controller (3) into (1), it obtains that

$$e^{(n)} + k_1 e^{(n-1)} + \cdots + k_{n-1}\dot{e} + k_n e = 0 . \tag{4}$$

If $k_i, i = 1,2,...,n$ are chosen to correspond to the coefficients of a Hurwitz polynomial, that is a polynomial whose roots lie strictly in the open left half of the complex plane, then it implies that $\lim_{t\to\infty} e(t) = 0$ [1]. However, the system dynamics is always unknown; the ideal controller u^* can not be implemented.

Rewriting (1), the nominal model of the nonlinear dynamic system can be represented as follows

$$\ddot{x} = f_n(\mathbf{x}) + u \tag{5}$$

where $f_n(\mathbf{x})$ is a mapping that represents the nominal behavior of $f(\mathbf{x})$. If uncertainties occur, i.e., the parameters of the system deviate from the nominal value and/or the external disturbance is added into the system, the controlled system can be modified as

$$x^{(n)} = f_n(\mathbf{x}) + \Delta f(\mathbf{x}) + u + d = f_n(\mathbf{x}) + u + z \tag{6}$$

where d is the external disturbance, $\Delta f(\mathbf{x})$ denotes the system uncertainties, and z is called the lumped uncertainty which defined as $z = \Delta f(\mathbf{x}) + d$ with the assumption $|z| \le Z$, in which Z is a given positive constant. A sliding surface is defined as

$$s = e^{(n-1)} + k_1 e^{(n-2)} + \ldots + k_{n-1} e + k_n \int_0^t e(\tau) d\tau . \tag{7}$$

The sliding-mode control law is given as [1]

$$u_{sc} = u_{eq} + u_{ht} \tag{8}$$

where the equivalent controller u_{eq} is represented as

$$u_{eq} = -f_n(\mathbf{x}) + x_c^{(n)} + k_1 e^{(n-1)} + \cdots + k_{n-1}\dot{e} + k_n e \tag{9}$$

and the hitting controller u_{ht} is designed to guarantee the system stability as

$$u_{ht} = Z\,\mathrm{sgn}(s) \tag{10}$$

where $\mathrm{sgn}(\cdot)$ is the sign function. Substituting (8), (9) and (10) into (6) yields

$$e^{(n)} + k_1 e^{(n-1)} + \cdots + k_{n-1}\dot{e} + k_n e = -z - Z\,\mathrm{sgn}(s) = \dot{s} . \tag{11}$$

An important concept of sliding-mode control is to make the system satisfy the reaching condition and guarantee sliding condition. Consider the candidate Lyapunov function in the following form as

$$V = \frac{1}{2} s^2 . \tag{12}$$

Differentiating (12) with respect to time and using (11) obtain

$$\begin{aligned} \dot{V}_1 = s\dot{s} &= -zs - Z|s| \\ &\le |z||s| - Z|s| \\ &= -(Z - |z|)|s| \le 0 . \end{aligned} \tag{13}$$

In summary, the sliding-mode controller in (8) can guarantee the stability in the sense of the Lyapunov theorem [1]. However, large control gain Z is often required in order to minimize time needed to reach the switching surface from the initial state. A conservative control law with large control gain Z is usually considered, but unnecessary jumping movement between the switching surface may yield and cause an outcome of large amount of chattering. The chattering phenomena in control efforts will wear the bearing mechanism and excite unmodelled dynamics.

III. CAWNNC System Design

In this paper, the chattering-free adaptive wavelet neural network control (CAWNNC) system is designed as shown in Fig. 1, where the controller output is defined as

$$u = \hat{u}_{wn} + u_{sc} . \tag{14}$$

The neural controller $\hat{u}_{wn}$ uses a FWNN to approximate the ideal controller u^*, and the smooth compensator u_{sc} is utilized to compensate the approximation error between neural controller and ideal controller. The descriptions of design steps are depicted as follows:

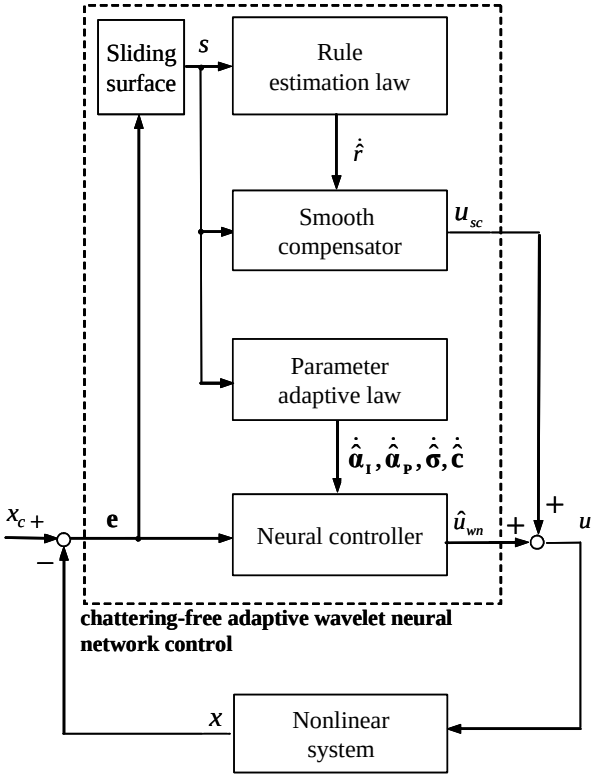

Fig. 1. CAWNNC for a class of nonlinear system.

A. Description of FWNN

The network structure of the proposed FWNN can be considered as multi-layer feedforward neural network as shown in Fig. 2. Assume that there are *m* rules in FWNN can be described as

Rule *i*: If e is A_1^i and $\dot{e}$ is A_2^i … and $e^{(n-1)}$ is A_n^i,

Then u_{wn} is $\alpha_i \psi_i(\mathbf{z})$ (15)

where $\mathbf{e} = [e\ \dot{e} \dots e^{(n-1)}]^T$ and u_{wn} are the input and output variables of FWNN, respectively, u_{wn} are the linguistic terms characterized by their corresponding fuzzy membership functions of the fuzzy sets, and $\alpha_i \psi_i(\mathbf{z})$ is the output weight. $\psi_i(\mathbf{z}) = \prod_{k=1}^{n}(1-\omega_{ki}^2 z_k^2)$ is defined as the "Mexican hat" mother wavelet function. Then, the FWNN performs the mappings according to

$$u_{wn} = \sum_{i=1}^{m} \alpha_i \psi_i(\mathbf{z}) \phi_i(\boldsymbol{\sigma}_i, \| \mathbf{e} - \mathbf{c}_i \|) \tag{16}$$

where $\boldsymbol{\sigma}_i = [\sigma_{1i}\ \sigma_{2i} \dots \sigma_{ni}]$ and $\mathbf{c}_i = [c_{1i}\ c_{2i} \dots c_{ni}]^T$ are the inverse of width and center vectors of the Gaussian membership, respectively. The Gaussian membership ϕ_i represents as

$$\phi_i(\boldsymbol{\sigma}_i, \| e - \mathbf{c}_i \|) = \prod_{j=1}^{n} \exp[-(e^{(j-1)} - c_{ji})^2 \sigma_{ji}^{\ 2}] \tag{17}$$

For ease of notation, (16) can be expressed in a compact vector form as

$$u_{wn} = \boldsymbol{\alpha}^T \boldsymbol{\Theta}(\mathbf{e}, \boldsymbol{\sigma}, \mathbf{c}) \tag{18}$$

where $\boldsymbol{\alpha} = [\alpha_1\ \alpha_2 \dots \alpha_m]^T$, $\boldsymbol{\Theta} = [\psi_1\phi_1\ \psi_2\phi_2 \dots \psi_m\phi_m]^T$, $\boldsymbol{\sigma} = [\boldsymbol{\sigma}_1\ \boldsymbol{\sigma}_2 \dots \boldsymbol{\sigma}_m]^T$ and $\mathbf{c} = [\mathbf{c}_1\ \mathbf{c}_2 \dots \mathbf{c}_m]^T$. This implies that there is a FWNN of (18) that can uniformly approximate an ideal controller. There exists ideal weight vectors so that [9]

$$u^* = \boldsymbol{\alpha}^{*T} \boldsymbol{\Theta}^*(\mathbf{e}, \boldsymbol{\sigma}^*, \mathbf{c}^*) + \Delta \tag{19}$$

where $\boldsymbol{\alpha}^*$ and $\boldsymbol{\Theta}^*$ are optimal parameter vectors of $\boldsymbol{\alpha}$ and $\boldsymbol{\Theta}$, respectively; $\boldsymbol{\sigma}^*$ and $\mathbf{c}^*$ are optimal parameter vectors of $\boldsymbol{\sigma}$ and $\mathbf{c}$, respectively; and Δ is the approximation error. However, the optimal parameter vectors are unknown, so it is necessary to estimate the values. Define an estimation function

$$\hat{u}_{wn} = \hat{\boldsymbol{\alpha}}^T \hat{\boldsymbol{\Theta}}(\mathbf{e}, \hat{\boldsymbol{\sigma}}, \hat{\mathbf{c}}) \tag{20}$$

where $\hat{\boldsymbol{\alpha}}$ and $\hat{\boldsymbol{\Theta}}$ are optimal parameter vectors of $\boldsymbol{\alpha}$ and $\boldsymbol{\Theta}$, respectively; and $\hat{\boldsymbol{\sigma}}$ and $\hat{\mathbf{c}}$ are optimal parameter vectors of $\boldsymbol{\sigma}$ and $\mathbf{c}$, respectively. Define the estimation error as

$$\begin{aligned} \tilde{u} &= u^* - \hat{u}_{wn} = \boldsymbol{\alpha}^{*T} \boldsymbol{\Theta}^* - \hat{\boldsymbol{\alpha}}^T \hat{\boldsymbol{\Theta}} + \Delta \\ &= \tilde{\boldsymbol{\alpha}}^T \tilde{\boldsymbol{\Theta}} + \hat{\boldsymbol{\alpha}}^T \tilde{\boldsymbol{\Theta}} + \tilde{\boldsymbol{\alpha}}^T \hat{\boldsymbol{\Theta}} + \Delta \end{aligned} \tag{21}$$

where $\tilde{\boldsymbol{\alpha}} = \boldsymbol{\alpha}^* - \hat{\boldsymbol{\alpha}}$ and $\tilde{\boldsymbol{\Theta}} = \boldsymbol{\Theta}^* - \hat{\boldsymbol{\Theta}}$. In order to deduce the adaptive law for mean and variance later, it is necessarily to derive the value of $\tilde{\boldsymbol{\Theta}}$. To achieve this goal, the Taylor expansion linearization technique is employed to transform the nonlinear function into a partially linear form, such that [11]

$$\tilde{\boldsymbol{\Theta}} = \mathbf{A}^T \tilde{\boldsymbol{\sigma}} + \mathbf{B}^T \tilde{\mathbf{c}} + \mathbf{h} \tag{22}$$

where $\tilde{\boldsymbol{\sigma}} = \boldsymbol{\sigma}^* - \hat{\boldsymbol{\sigma}}$, $\tilde{\mathbf{c}} = \mathbf{c}^* - \hat{\mathbf{c}}$, $\mathbf{A} = \left[\frac{\partial \Theta_1}{\partial \boldsymbol{\sigma}} \ \cdots \ \frac{\partial \Theta_m}{\partial \boldsymbol{\sigma}} \right]\Big|_{\boldsymbol{\sigma}=\hat{\boldsymbol{\sigma}}}$, $\mathbf{B} = \left[\frac{\partial \Theta_1}{\partial \mathbf{c}} \ \cdots \ \frac{\partial \Theta_m}{\partial \mathbf{c}} \right]\Big|_{\mathbf{c}=\hat{\mathbf{c}}}$, and $\mathbf{h}$ is the high order terms of expansion. Substitute (22) into (21), it can obtain that

$$\begin{aligned} \tilde{u} &= \tilde{\boldsymbol{\alpha}}^T \tilde{\boldsymbol{\Theta}} + \hat{\boldsymbol{\alpha}}^T (\mathbf{A}^T \tilde{\boldsymbol{\sigma}} + \mathbf{B}^T \tilde{\mathbf{c}} + \mathbf{h}) + \tilde{\boldsymbol{\alpha}}^T \hat{\boldsymbol{\Theta}} + \Delta \\ &= \tilde{\boldsymbol{\alpha}}^T \hat{\boldsymbol{\Theta}} + \tilde{\boldsymbol{\sigma}}^T \mathbf{A} \hat{\boldsymbol{\alpha}} + \tilde{\mathbf{c}}^T \mathbf{B} \hat{\boldsymbol{\alpha}} + \hat{\boldsymbol{\alpha}}^T \mathbf{h} + \tilde{\boldsymbol{\alpha}}^T \tilde{\boldsymbol{\Theta}} + \Delta \end{aligned} \tag{23}$$

where $\hat{\boldsymbol{\alpha}}^T \mathbf{A}^T \tilde{\boldsymbol{\sigma}} = \tilde{\boldsymbol{\sigma}}^T \mathbf{A} \hat{\boldsymbol{\alpha}}$ and $\hat{\boldsymbol{\alpha}}^T \mathbf{B}^T \tilde{\mathbf{c}} = \tilde{\mathbf{c}}^T \mathbf{B} \hat{\boldsymbol{\alpha}}$ are used since they are scalars. To speed up the convergence of FWNN learning, the optimal parameter vector $\boldsymbol{\alpha}^*$ is decomposed into two parts as [19]

$$\boldsymbol{\alpha}^* = \eta_P \boldsymbol{\alpha}_{\mathbf{P}}^* + \eta_I \boldsymbol{\alpha}_{\mathbf{I}}^* \tag{24}$$

where η_P and η_I are positive constants, and $\boldsymbol{\alpha}_{\mathbf{P}}^*$ and $\boldsymbol{\alpha}_{\mathbf{I}}^*$ are the proportional and integral terms of $\boldsymbol{\alpha}^*$, respectively, and $\boldsymbol{\alpha}_{\mathbf{I}}^* = \int_0^t \boldsymbol{\alpha}_{\mathbf{P}}^* \, d\tau$. The estimation parameter vector $\hat{\boldsymbol{\alpha}}$ is decomposed into two parts as [19]

$$\hat{\boldsymbol{\alpha}} = \eta_P \hat{\boldsymbol{\alpha}}_{\mathbf{P}} + \eta_I \hat{\boldsymbol{\alpha}}_{\mathbf{I}} \tag{25}$$

where $\hat{\boldsymbol{\alpha}}_{\mathbf{P}}$ and $\hat{\boldsymbol{\alpha}}_{\mathbf{I}}$ are the proportional and integral terms of $\hat{\boldsymbol{\alpha}}$, respectively, and $\hat{\boldsymbol{\alpha}}_{\mathbf{I}} = \int_0^t \hat{\boldsymbol{\alpha}}_{\mathbf{P}} \, d\tau$. Thus, $\tilde{\boldsymbol{\alpha}}$ can be expressed as

$$\tilde{\boldsymbol{\alpha}} = \eta_I \tilde{\boldsymbol{\alpha}}_{\mathbf{I}} - \eta_P \hat{\boldsymbol{\alpha}}_{\mathbf{P}} + \eta_P \boldsymbol{\alpha}_{\mathbf{P}}^* \tag{26}$$

where $\tilde{\boldsymbol{\alpha}}_{\mathbf{I}} = \boldsymbol{\alpha}_{\mathbf{I}}^* - \hat{\boldsymbol{\alpha}}_{\mathbf{I}}$. Substituting (26) into (23) obtains

$$\begin{aligned} \tilde{u} &= (\eta_I \tilde{\boldsymbol{\alpha}}_{\mathbf{I}} - \eta_P \hat{\boldsymbol{\alpha}}_{\mathbf{P}} + \eta_P \boldsymbol{\alpha}_{\mathbf{P}}^*)^T \hat{\boldsymbol{\Theta}} \\ &\quad + \tilde{\boldsymbol{\sigma}}^T \mathbf{A} \hat{\boldsymbol{\alpha}} + \tilde{\mathbf{c}}^T \mathbf{B} \hat{\boldsymbol{\alpha}} + \hat{\boldsymbol{\alpha}}^T \mathbf{h} + \tilde{\boldsymbol{\alpha}}^T \tilde{\boldsymbol{\Theta}} + \Delta \\ &= \eta_I \tilde{\boldsymbol{\alpha}}_{\mathbf{I}}^T \hat{\boldsymbol{\Theta}} - \eta_P \hat{\boldsymbol{\alpha}}_{\mathbf{P}}^T \hat{\boldsymbol{\Theta}} + \tilde{\boldsymbol{\sigma}}^T \mathbf{A} \hat{\boldsymbol{\alpha}} + \tilde{\mathbf{c}}^T \mathbf{B} \hat{\boldsymbol{\alpha}} + \varepsilon \end{aligned} \tag{27}$$

where the uncertain term $\varepsilon = \eta_P \boldsymbol{\alpha}_{\mathbf{P}}^{*T} \hat{\boldsymbol{\Theta}} + \hat{\boldsymbol{\alpha}}^T \mathbf{h} + \tilde{\boldsymbol{\alpha}}^T \tilde{\boldsymbol{\Theta}} + \Delta$.

B. Smooth compensator

Assume that the smooth compensator has 3 fuzzy rules in a rule base as given in the following form [20]

Rule 1: If s is PE, then u_{sc} is P (28)

Rule 2: If s is ZO, then u_{sc} is Z (29)

Rule 3: If s is NE, then u_{sc} is N (30)

where the triangular-typed functions and singletons are used to define the membership functions of IF-part and THEN-part, which are depicted in Figs. 3(a) and 3(b), respectively. The defuzzification of the output is accomplished by the method of center-of-gravity

$$u_{sc} = \frac{\sum_{i=1}^{3} r_i w_i}{\sum_{i=1}^{3} w_i} = r_1 w_1 + r_2 w_2 + r_3 w_3 \tag{31}$$

where $0 \le w_1 \le 1$, $0 \le w_2 \le 1$ and $0 \le w_3 \le 1$ are the firing strengths of rules 1, 2, and 3, respectively; and the relation $w_1 + w_2 + w_3 = 1$ is valid according to the special case of triangular membership function-based fuzzy system. In order to reduce the computation loading, let $r_1 = \hat{r}$, $r_2 = 0$ and $r_3 = -\hat{r}$. Hence, for any value of input x, only one of four conditions will occur according to Fig. 3(a) as [21]

Condition1: Only rule 1 is triggered ($x > x_a$, $w_1 = 1$, $w_2 = w_3 = 0$)

$$u_{sc} = r_1 = \hat{r} \tag{32}$$

Condition2: Rules 1 and 2 are triggered simultaneously. ($0 < x \le x_a$, $0 < w_1, w_2 \le 1$, $w_3 = 0$)

$$u_{sc} = r_1 w_1 = \hat{r} w_1 \tag{33}$$

Condition3: Rules 2 and 3 are triggered simultaneously. ($x_b < x \le 0$, $w_1 = 0$, $0 < w_2, w_3 \le 1$)

$$u_{sc} = r_3 w_3 = -\hat{r} w_3 \tag{34}$$

Condition 4: Only rule 3 is triggered. ($x \le x_b$, $w_1 = w_2 = 0$, $w_3 = 1$)

$$u_{sc} = r_3 = -\hat{r} \tag{35}$$

Then, the (31)-(34) can be rewritten as

$$u_{sc} = \hat{r}(w_1 - w_3) \tag{36}$$

Moreover, it can see that [21]

$$s(w_1 - w_3) = |s|\,|(w_1 - w_3)| \ge 0 \tag{37}$$

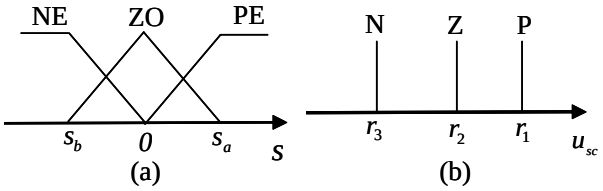

Fig. 3. (a) input fuzzy sets. (b) output fuzzy sets.

C. On-line learning algorithm

Substituting (14) into (1) and using (3), yields

$$u^* - \hat{u}_{wn} - u_{sc} = \dot{s} \tag{38}$$

By using the approximation property (27), (38) can be rewritten as

$$\dot{s} = \eta_I \tilde{\boldsymbol{\alpha}}_{\mathbf{I}}^T \hat{\boldsymbol{\Theta}} - \eta_P \hat{\boldsymbol{\alpha}}_{\mathbf{P}}^T \hat{\boldsymbol{\Theta}} + \tilde{\boldsymbol{\sigma}}^T \mathbf{A} \hat{\boldsymbol{\alpha}} + \tilde{\mathbf{c}}^T \mathbf{B} \hat{\boldsymbol{\alpha}} + \varepsilon - u_{sc}. \tag{39}$$

To proof the stability of the CAWNNC system, define a Lyapunov function candidate in the following form

$$V_a = \frac{1}{2} s^2 + \frac{\eta_I}{2} \tilde{\boldsymbol{\alpha}}_{\mathbf{I}}^T \tilde{\boldsymbol{\alpha}}_{\mathbf{I}} + \frac{1}{2\eta_\sigma} \tilde{\boldsymbol{\sigma}}^T \tilde{\boldsymbol{\sigma}} + \frac{1}{2\eta_c} \tilde{\mathbf{c}}^T \tilde{\mathbf{c}} \tag{40}$$

where η_σ and η_c are the learning rates with positive constants. Differentiating (40) with respect to time and using (39), it is obtained that

$$\begin{aligned} \dot{V}_a &= s\dot{s} + \eta_I \tilde{\boldsymbol{\alpha}}_{\mathbf{I}}^T \dot{\tilde{\boldsymbol{\alpha}}}_{\mathbf{I}} + \frac{1}{\eta_\sigma} \tilde{\boldsymbol{\sigma}}^T \dot{\tilde{\boldsymbol{\sigma}}} + \frac{1}{\eta_c} \tilde{\mathbf{c}}^T \dot{\tilde{\mathbf{c}}} \\ &= \eta_I \tilde{\boldsymbol{\alpha}}_{\mathbf{I}}^T (s\hat{\boldsymbol{\Theta}} + \dot{\tilde{\boldsymbol{\alpha}}}_{\mathbf{I}}) + \tilde{\boldsymbol{\sigma}}^T (s\mathbf{A}\hat{\boldsymbol{\alpha}} + \frac{\dot{\tilde{\boldsymbol{\sigma}}}}{\eta_\sigma}) + \tilde{\mathbf{c}}^T (s\mathbf{B}\hat{\boldsymbol{\alpha}} + \frac{\dot{\tilde{\mathbf{c}}}}{\eta_c}) \\ &\quad - s\eta_P \hat{\boldsymbol{\alpha}}_{\mathbf{P}}^T \hat{\boldsymbol{\Theta}} + s(\varepsilon - u_{sc}) \end{aligned} \tag{41}$$

If the parameter adaptive laws are selected as

$$\hat{\boldsymbol{\alpha}}_{\mathbf{P}} = s\hat{\boldsymbol{\Theta}} \tag{42}$$

$$\dot{\hat{\boldsymbol{\alpha}}}_{\mathbf{I}} = -\dot{\tilde{\boldsymbol{\alpha}}}_{\mathbf{I}} = s\hat{\boldsymbol{\Theta}} \tag{43}$$

$$\dot{\hat{\boldsymbol{\sigma}}} = -\dot{\tilde{\boldsymbol{\sigma}}} = \eta_\sigma s\mathbf{A}\hat{\boldsymbol{\alpha}} \tag{44}$$

$$\dot{\hat{\mathbf{c}}} = -\dot{\tilde{\mathbf{c}}} = \eta_c s\mathbf{B}\hat{\boldsymbol{\alpha}} \tag{45}$$

and the smooth compensator is design as (36), then (41) can be rewritten as

$$\begin{aligned} \dot{V}_a &= -\eta_P \hat{\boldsymbol{\alpha}}_{\mathbf{P}}^T \hat{\boldsymbol{\alpha}}_{\mathbf{P}} + s(\varepsilon - u_{sc}) \\ &\le -\eta_P \hat{\boldsymbol{\alpha}}_{\mathbf{P}}^T \hat{\boldsymbol{\alpha}}_{\mathbf{P}} + |s||\varepsilon| - \hat{r}s(w_1 - w_3) \\ &\le |s||\varepsilon| - \hat{r}|s||w_1 - w_3| \\ &= -|s||w_1 - w_3|(\hat{r} - \frac{|\varepsilon|}{|w_1 - w_3|}) \end{aligned} \tag{46}$$

If the following inequality

$$\hat{r} > \frac{|\varepsilon|}{|w_1 - w_3|} \tag{47}$$

holds, then the sliding condition $\dot{V}_a \le 0$ can be satisfied. Owing to the unknown lumped uncertainties, the value $\hat{r}$ cannot be exactly obtained in advance for practical applications. According to (47), there exists an ideal value r^* as follows to achieve minimum value and match the sliding condition:

$$r^* = \frac{|\varepsilon|}{|w_1 - w_3|} + \kappa \tag{48}$$

where κ is a positive constant. Thus, a simple adaptive algorithm is utilized in this study to estimate the ideal value of r^*, and its estimated error is defined as

$$\tilde{r} = r^* - \hat{r} \tag{49}$$

where $\hat{r}$ is the estimated value of the optimal value of r^*. Then, define a new Lyapunov function candidate in the following form

$$V_b = \frac{1}{2} s^2 + \frac{\eta_I}{2} \tilde{\boldsymbol{\alpha}}_{\mathbf{I}}^T \tilde{\boldsymbol{\alpha}}_{\mathbf{I}} + \frac{1}{2\eta_\sigma} \tilde{\boldsymbol{\sigma}}^T \tilde{\boldsymbol{\sigma}} + \frac{1}{2\eta_c} \tilde{\mathbf{c}}^T \tilde{\mathbf{c}} + \frac{1}{2\eta_r} \tilde{r}^2 \tag{50}$$

where η_r is the learning rate with a positive constant. Differentiating (50) with respect to time and using (39) and (42)-(45), it is obtained that

$$\begin{aligned}\dot{V}_a &= s\dot{s} + \eta_I \tilde{\boldsymbol{\alpha}}_{\mathbf{I}}^T \dot{\tilde{\boldsymbol{\alpha}}}_{\mathbf{I}} + \frac{1}{\eta_\sigma}\tilde{\boldsymbol{\sigma}}^T\dot{\tilde{\boldsymbol{\sigma}}} + \frac{1}{\eta_c}\tilde{\mathbf{c}}^T\dot{\tilde{\mathbf{c}}} + \frac{1}{\eta_r}\tilde{r}\dot{\tilde{r}} \\ &= -\eta_P \hat{\boldsymbol{\alpha}}_{\mathbf{p}}^T \hat{\boldsymbol{\alpha}}_{\mathbf{p}} + s\varepsilon - \hat{r}s(w_1 - w_3) + \frac{1}{\eta_r}\tilde{r}\dot{\tilde{r}} \\ &\le s\varepsilon - \hat{r}s(w_1 - w_3) + \frac{1}{\eta_r}\tilde{r}\dot{\tilde{r}} \\ &\le |s||\varepsilon| - \hat{r}s(w_1 - w_3) + r^* s(w_1 - w_3) - r^* s(w_1 - w_3) + \frac{1}{\eta_r}\tilde{r}\dot{\tilde{r}} \\ &= |s||\varepsilon| + \tilde{r}s(w_1 - w_3) - r^* s(w_1 - w_3) + \frac{1}{\eta_r}\tilde{r}\dot{\tilde{r}} \\ &= \tilde{r}[s(w_1 - w_3) + \frac{1}{\eta_r}\dot{\tilde{r}}] + |s||\varepsilon| - r^*|s||w_1 - w_3| \end{aligned} \quad (51)$$

Choose the rule estimation laws as

$$\dot{\hat{r}} = -\dot{\tilde{r}} = \eta_r s(w_1 - w_3) \quad (52)$$

and using (48), (51) becomes

$$\begin{aligned}\dot{V}_b &= |s||\varepsilon| - |s|(|\varepsilon| + \kappa|w_1 - w_3|) \\ &= -\kappa|s||w_1 - w_3| \le 0 \end{aligned} \quad (53)$$

As a result, the stability of the proposed CAWNNC system can be guaranteed [1].

In the following, the design steps of CAWNNC are summarized as follows:

Step 1: The tracking error e and the sliding surface s are given in (2) and (7), respectively.

Step 2: $\hat{u}_{wn}$ is given as $\hat{\boldsymbol{\alpha}}^T\hat{\boldsymbol{\Theta}}(\mathbf{e}, \hat{\boldsymbol{\sigma}}, \hat{\mathbf{c}})$, where $\hat{\boldsymbol{\alpha}}$ is estimated by (42) and (43), simultaneously, and $\hat{\boldsymbol{\sigma}}$ and $\hat{\mathbf{c}}$ are estimated by (44) and (45), respectively.

Step 3: u_{sc} is given as $\hat{r}(w_1 - w_3)$, where $\hat{r}$ is estimated by (52).

Step 4: The control law is given as $u = \hat{u}_{wn} + u_{sc}$.

Step 5: Return to Step 1.

IV. Simulation Results

In this section, the proposed CAWNNC system is applied to control two chaotic nonlinear systems to verify its effectiveness. Chaotic nonlinear systems have been studied and known to exhibit complex dynamical behavior. The interest in chaotic systems lies mostly upon their complex, unpredictable behavior, and extreme sensitivity to initial conditions as well as parameter variations [22]-[27]. For control engineers, control of a chaotic system has become a significant research topic in physics, mathematics and engineering communities. It should be emphasized that the development of the CAWNNC does not need to know the system dynamics of the controlled system. For practical implementation, the controller parameters of CAWNNC can be online tuned by the proposed adaptive laws.

Example 1: Consider a second-order chaotic system such as the Duffing's equation describing a special nonlinear circuit or a pendulum moving in a viscous medium [22]

$$\ddot{x} = -p\dot{x} - p_1 x - p_2 x^3 + q\cos(\omega t) + u = f(\mathbf{x}) + u \quad (54)$$

where $\mathbf{x} = [x\ \dot{x}]^T$ is the state vector of the system, t is the time variable; w is the frequency, p, p_1, p_2 and q are real constants, $f(\mathbf{x}) = -p\dot{x} - p_1 x - p_2 x^3 + q\cos(\omega t)$ is the system dynamic function, and u is the control effort. Depending on the choices of these constants, the solutions of system (54) may display complex phenomena, including various periodic orbits behaviors and some chaotic behaviors. To observe these complex phenomena, the open-loop system behavior with u=0 was simulated with $p = 0.4$, $p_1 = -1.1$, $p_2 = 1.0$ and $\omega = 1.8$. The phase plane plots with an initial condition (0, 0) are shown in Figs. 4(a) and 4(b) for $q = 2.1$ (chaotic) and $q = 7.0$ (period 1), respectively. It is shown that the uncontrolled chaotic dynamic system has different chaotic trajectories for different values of q.

The control parameters of the proposed CAWNNC scheme are selected as $k_1 = 2$, $k_2 = 1$, $\eta_I = \eta_P = 20$ and $\eta_\sigma = \eta_c = \eta_r = 1$. These parameters are selected through trails. All the gains in the CAWNNC are chosen to achieve good transient control performance in the simulation considering the requirement of stability and possible operating conditions. The simulation results of CAWNNC for $q = 2.1$ and $q = 7.0$ are shown in Figs. 5 and 6, respectively. The tracking responses of state x are shown in Figs. 5(a) and 6(a); the tracking responses of state $\dot{x}$ are shown in Figs. 5(b) and 6(b); and the associated control efforts are shown Figs. 5(c) and 6(c) for $q = 2.1$ and $q = 7.0$, respectively. From these simulation results, it can be seen that robust tracking performance can be achieved without any knowledge of system dynamic functions.

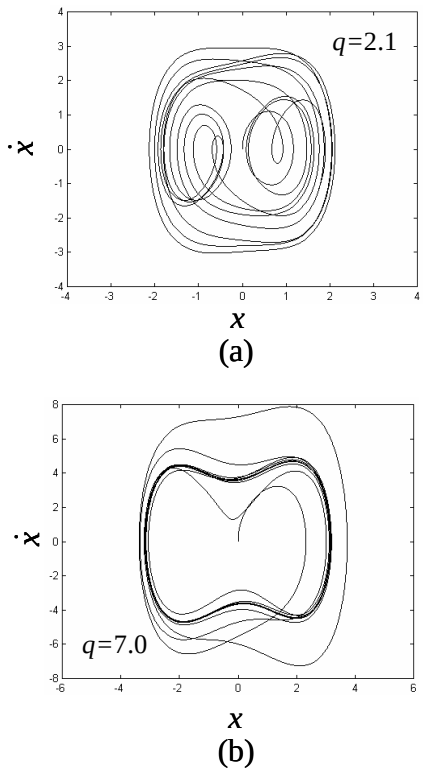

Fig. 4. Phase plane of uncontrolled chaotic dynamic system.

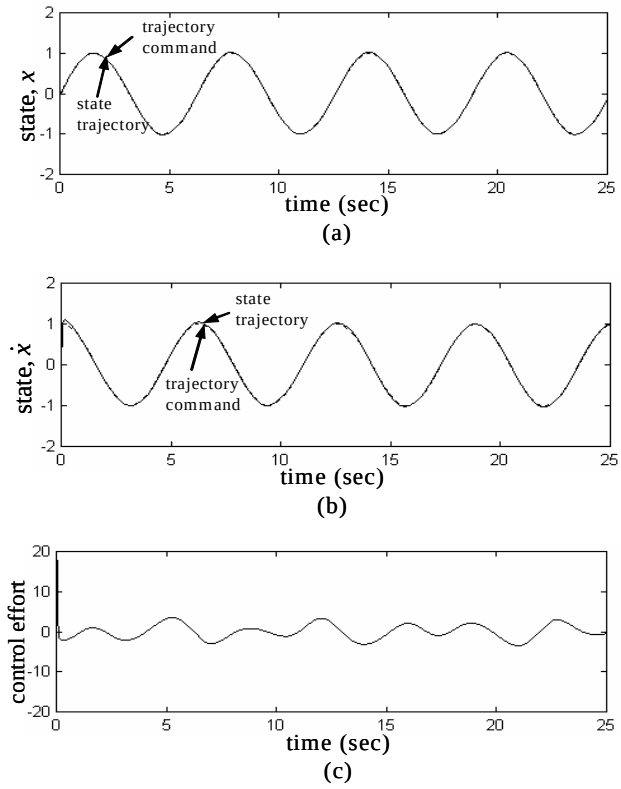

Fig. 5. Simulation results of CAWNNC for $q = 2.1$.

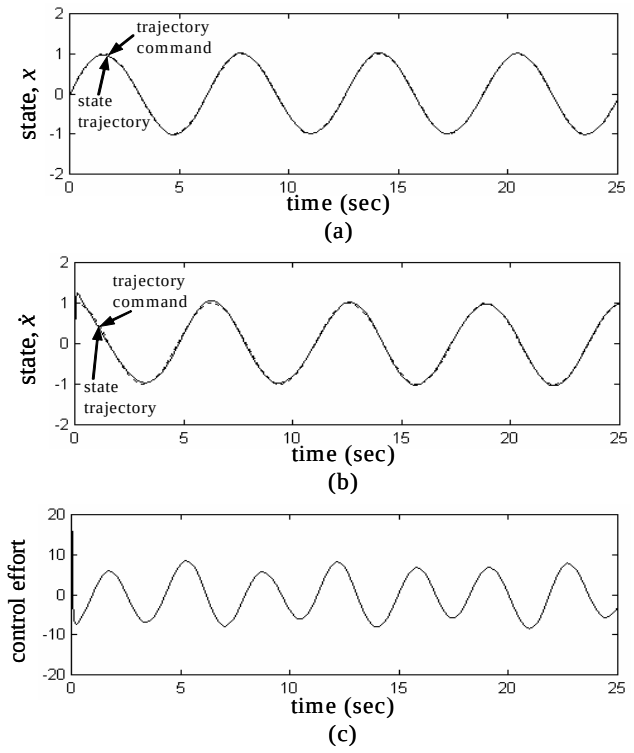

Fig. 6. Simulation results of CAWNNC for $q = 7.0$.

Example 2: A third-order Chua's chaotic circuit, as shown in Fig. 7, is a simple electronic system that consists of one linear resistor (R), two capacitors (C_1, C_2), one inductor (L), and one nonlinear resistor (λ). It has been shown to own very rich nonlinear dynamics such as chaos and bifurcations. The dynamic equations of Chua's circuit are written as [26]

$$\dot{v}_{C_1} = \frac{1}{C_1}\left(\frac{1}{R}(v_{C_2} - v_{C_1}) - \lambda(v_{C_2})\right) \tag{54}$$

$$\dot{v}_{C_2} = \frac{1}{C_2}\left(\frac{1}{R}(v_{C_1} - v_{C_2}) + i_L\right) \tag{55}$$

$$\dot{i}_L = \frac{1}{L}(-v_{C_1} - R_0 i_L) \tag{56}$$

where the voltages v_{C_1}, v_{C_2} and current i_L are state variables, R_0 is a constant, and λ denotes the nonlinear resistor, which is a function of the voltage across the two terminals of C_1. The λ is defined as a cubic function as

$$\lambda(v_{C_1}) = a v_{C_1} + c v_{C_1}^3 \ (a < 0, c > 0). \tag{57}$$

The state equations in (54)~(56) are not in the standard canonical form in (1). Therefore, a linear transformation is needed to transform them into the form of (1). The dynamic equations of transformed Chua's circuit can be rewritten as [26]

$$x^{(3)} = f(\mathbf{x}) + u \tag{58}$$

where $\mathbf{x} = [x\ \dot{x}\ \ddot{x}]^T$ is the state vector of the system, the system dynamic function $f(\mathbf{x}) = \frac{14}{1805}x - \frac{168}{9025}\dot{x} + \frac{1}{38}\ddot{x} - \frac{2}{45}\left(\frac{28}{361}x + \frac{7}{95}\dot{x} + \ddot{x}\right)^3$ is the system dynamic function and u is the control effort.

The control parameters of the proposed CAWNNC scheme are selected as $k_1 = 3$, $k_2 = 3$, $k_3 = 1$, $\eta_I = \eta_P = 10$ and $\eta_\sigma = \eta_c = \eta_r = 1$. These parameters are selected through trails. All the gains in the CAWNNC are chosen to achieve good transient control performance in the simulation considering the requirement of stability and possible operating conditions. As $\eta_P = 0$, the learning algorithm of the proposed method is the same as conventional WNN-based adaptive control such as [11]. The simulation results of the CAWNNC to track a periodic sinusoidal command with $\eta_P = 0$ and $\eta_P = 10$ are shown in Figs. 8 and 9, respectively. The tracking responses of state x are shown in Figs. 8(a) and 9(a); the tracking responses of state $\dot{x}$ are shown in Figs. 8(b) and 9(b); the tracking responses of state $\ddot{x}$ are shown in Figs. 8(c) and 9(c); and the associated control efforts are shown Figs. 8(d) and 9(d) for $\eta_P = 0$ and $\eta_P = 10$, respectively. From the simulation results, it shows the convergence of controller parameter and tracking error converge be accelerated by the developed PI adaptation learning algorithm.

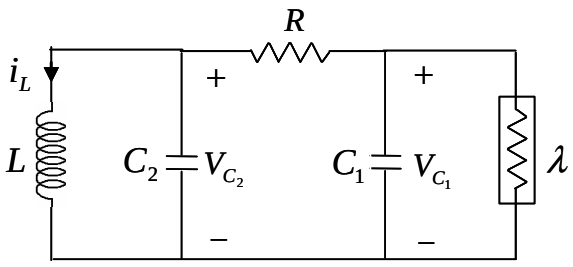

Fig. 7. Chua's chaotic circuit.

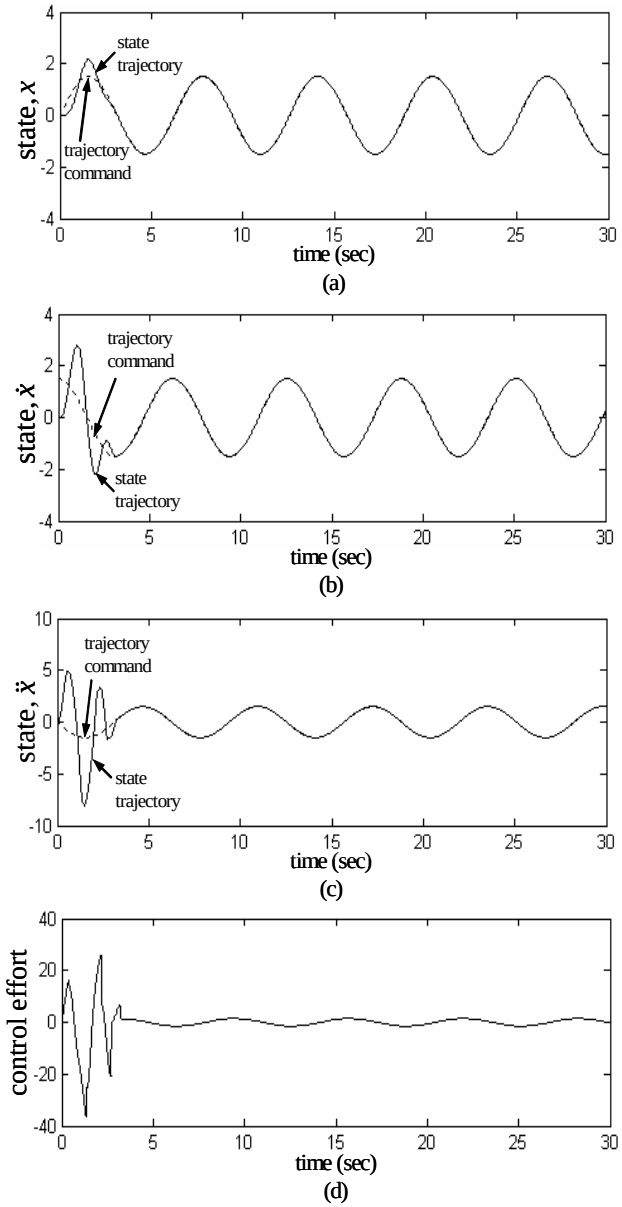

Fig. 8. Simulation results of CAWNNC with $\eta_P = 0$.

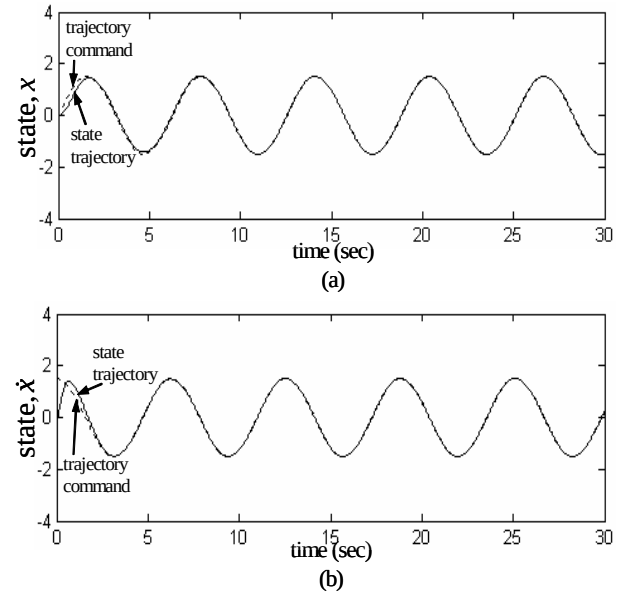

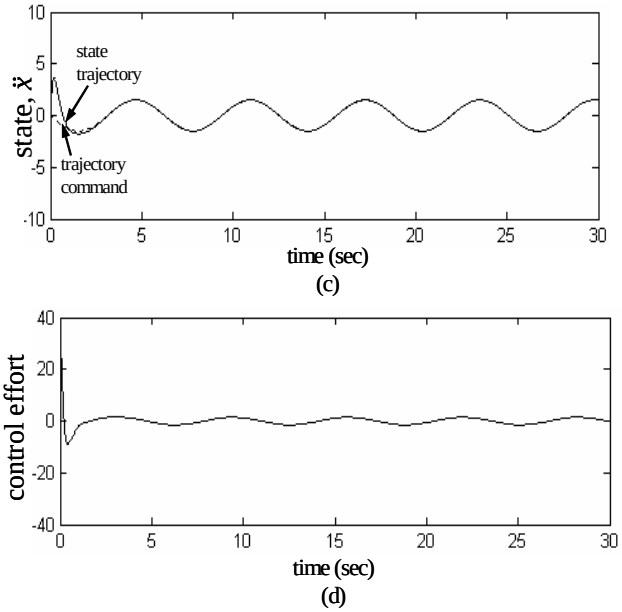

Fig. 9. Simulation results of CAWNNC with $\eta_P = 10$.

V. Conclusions

A chattering-free adaptive wavelet neural network control (CAWNNC) with a PI type learning algorithm is proposed. The stability is proven by Lyapunov function with the online parameter tuning laws are given to adjust the interconnection weights, dilation and translation parameters of wavelet functions. The effectiveness of the CAWNNC system is verified by some simulations. The main contributions of this paper are: (1) a learning algorithm with PI adaptation learning algorithm can achieve better tracking performance; and (2) the smooth compensator design uses a simple fuzzy system can remove completely the chattering phenomena.

Acknowledgment

The authors appreciate the partial financial support from the National Science Council of Republic of China under grant NSC 97-2221-E-216-029.

References

[1] J. J. E. Slotine and W. P. Li, *Applied Nonlinear Control*, Englewood Cliffs, NJ: Prentice Hall, 1991.

[2] O. Omidvar and D. L. Elliott, *Neural Systems for Control*, Academic Press 1997.

[3] C. M. Lin and C. F. Hsu, "Neural network hybrid control for antilock braking systems," *IEEE Trans. Neural Netw.*, vol. 14, no. 2, 2003, pp. 351-359.

[4] J. Q. Huang and F. L. Lewis, "Neural-network predictive control for nonlinear dynamic systems with time-delay," *IEEE Trans. Neural Netw.*, vol. 14, no. 2, 2003, pp. 377-389.

[5] C. M. Lin and C. F. Hsu, "Supervisory recurrent fuzzy neural network control of wing rock for slender delta wings, *IEEE Trans. Fuzzy Syst.*, vol. 12, no. 5, 2004, pp. 733-742.

[6] C. F. Hsu, C. M. Lin, and T. Y. Chen, "Neural-network-identification-based adaptive control of wing rock motion," *IEE Proc., Contr. Theory Appl.*, vol. 152, no.1, 2005, pp. 65-71.

[7] Q. Zhang and A. Benveniste, "Wavelet networks," *IEEE Trans. Neural Netw.*, vol. 37, no. 6, 1992, pp. 889-898.

[8] Q. Zhang, "Using wavelet network in nonparametric estimation," *IEEE Trans. Neural Netw.*, vol. 8, no. 2, 1997, pp. 227-236.

[9] S. A. Billings and H. L. Wei, "A new class of wavelet networks for nonlinear system identification," *IEEE Trans. Neural Netw.*, vol. 16, no. 4, 2005, pp. 862-874.

[10] C. D. Sousa, E. M. Hemerly, and R. K. H. Galvao, "Adaptive control for mobile robot using wavelet networks," *IEEE Trans. Syst., Man and Cybern., Pt B*, vol. 32, no. 4, 2002, pp. 493-504.

[11] C. K. Lin, "Adaptive tracking controller design for robotic systems using Gaussian wavelet networks," *IEE Proc., Contr. Theory Appl.*, vol. 149, no. 4, 2002, pp. 316-322.

[12] R. J. Wai and H. H. Chang, "Backstepping wavelet neural network control for indirect field-oriented induction motor drive," *IEEE Trans. Neural Netw.*, vol. 15, no. 2, 2004, pp. 367-382.

[13] C. F. Hsu, C. M. Lin, and T. T. Lee, "Wavelet adaptive backstepping control for a class of nonlinear systems," *IEEE Trans. Neural Netw.*, vol. 17, no. 5, 2006, pp. 1175-1183.

[14] C. M. Lin, K. N. Hung, and C. F. Hsu, "Adaptive neuro-wavelet control for switching power supplies," *IEEE Trans. Power Electronics*, vol. 22, no. 1, 2007, pp. 87-95.

[15] J. H. Park, S. J. Seo, and G. T. Park, "Robust adaptive fuzzy controller for nonlinear system using estimation of bounds for approximation errors," *Fuzzy Set Syst.*, vol. 133, no. 1, 2003, pp. 19-36.

[16] W. Y. Wang, M. L. Chan, C. C. J. Hsu, and T. T. Lee, "H^{∞} tracking-based sliding mode control for uncertain nonlinear systems via an adaptive fuzzy-neural approach," *IEEE Trans. Syst., Man and Cybern., Pt B*, vol. 32, no. 4, 2002, pp. 483-492.

[17] C. M. Lin, Y. F. Peng, and C. F. Hsu, "Robust cerebellar model articulation controller design for unknown nonlinear systems," *IEEE Trans. Circuits Systems II*, vol. 51, no. 7, 2004, pp. 354-358.

[18] Y. F. Peng and C. M. Lin, "Intelligent motion control of linear ultrasonic motor with H^{∞} tracking performance," *IET Control Theory Appl*, vol. 1, no. 1, 2007, pp. 9-17.

[19] N. Golea, A. Golea, and K. Benmahammed, "Fuzzy model reference adaptive control," *IEEE Trans. Fuzzy Syst.*, vol. 10, no. 4, 2002, pp. 436-444.

[20] J. R. Timothy, *Fuzzy Logic with Engineering Application*. NewYork: Mc-Graw Hill, 1995.

[21] R. J. Wai, "Fuzzy sliding-mode control using adaptive tuning technique," *IEEE Trans. Industrial Electronics*, vol. 54, no. 1, 2007, pp. 586-594.

[22] G. Chen and X. Dong, "On Feedback Control of Chaotic Continuous-Time Systems," *IEEE Trans. Circuits Syst. I*, vol. 40, no. 9, 1993, pp. 591-601.

[23] Y. C. Chang, "A robust tracking control for chaotic Chua's circuits via fuzzy approach," *IEEE Trans. Circuits Syst. I*, vol. 48, no. 7, 2001, pp. 889-895.

[24] Z. P. Jiang, "Advanced feedback control of the chaotic Duffing equation," *IEEE Trans. Circuits Syst. I*, vol. 49, no. 2, 2002, pp. 244-249.

[25] C. M. Lin and Y. F. Peng, "Adaptive CMAC-based supervisory control for uncertain nonlinear systems," *IEEE Trans. Syst., Man, Cybern. B*, vol. 34, no. 2, 2004, pp. 1248-1260.

[26] C. H. Wang, T. C. Lin, T. T. Lee, and H. L. Liu, "Adaptive hybrid intelligent control for uncertain nonlinear dynamical systems," *IEEE Trans. Syst., Man, Cybern. B*, vol. 32, no. 2, 2002, pp. 583-597.

[27] C. F. Hsu, "Self-organizing adaptive fuzzy neural control for a class of nonlinear systems," *IEEE Trans. Neural Netw.*, vol. 18, no. 4, 2007, pp. 1232-1241.

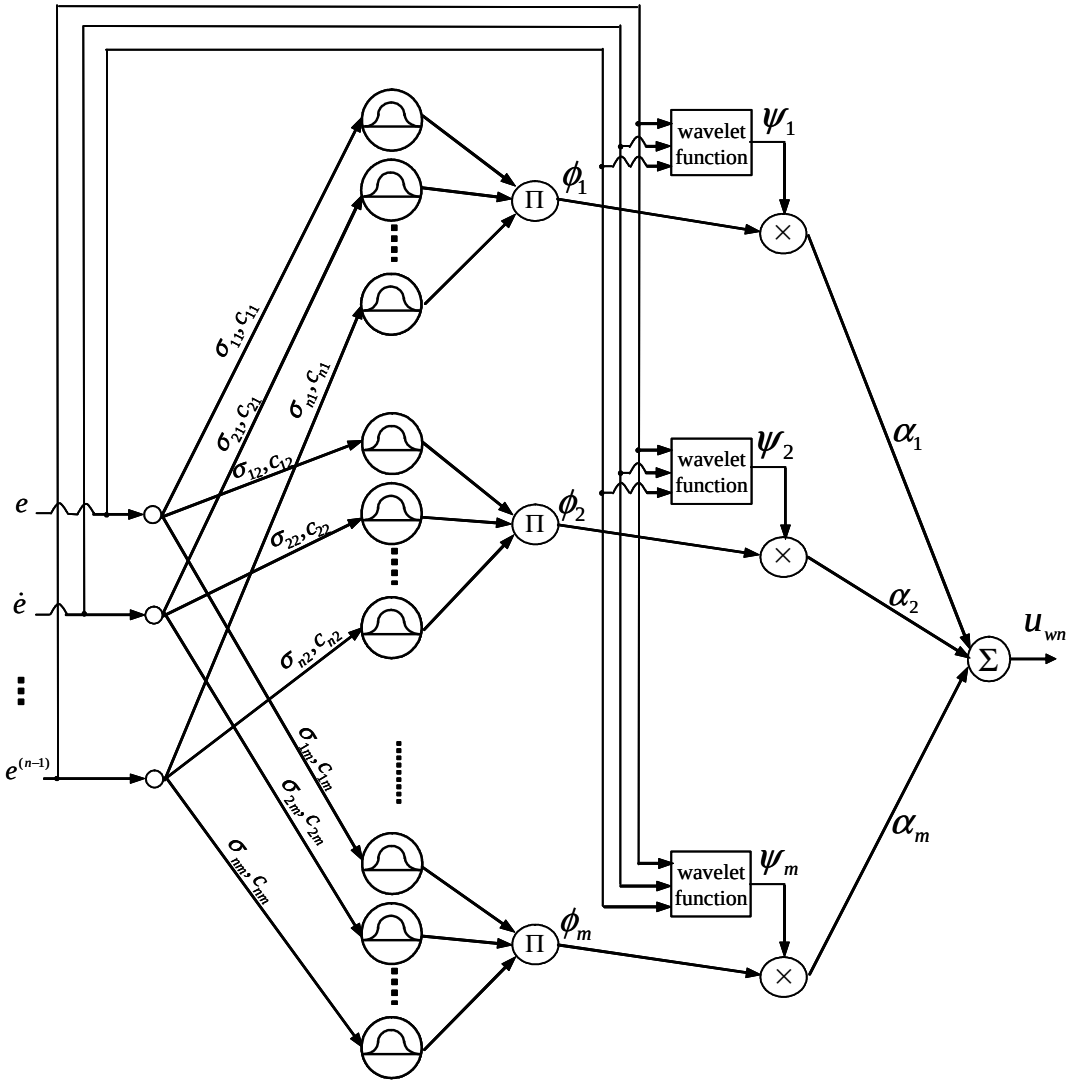

Fig. 2. Network structure of a FWNN.